Title

THE INFLUENCE OF COMBUSTION ON REYNOLDS STRESS IN A STRONGLY HEATED TURBULENT BOUNDARY LAYER

Authors
Cheng, R.K.
Ng, T.T.

Publication Date
1983-06-01

Lawrence Berkeley Laboratory

UNIVERSITY OF CALIFORNIA

ENERGY & ENVIRONMENT DIVISION

To be presented the 21st National Heat Transfer Conference, Seattle, WA, July 25, 1983

THE INFLUENCE OF COMBUSTION ON REYNOLDS STRESS IN A STRONGLY HEATED TURBULENT BOUNDARY LAYER

R.K. Cheng and T.T. Ng

June 1983

ENERGY AND ENVIRONMENT DIVISION

Prepared for the U.S. Department of Energy under Contract DE-AC03-76SF00098

LBL-16297

THE INFLUENCE OF COMBUSTION ON REYNOLDS STRESS IN A STRONGLY HEATED TURBULENT BOUNDARY LAYER

R. K. Cheng

Energy and Environment Division
Lawrence Berkeley Laboratory
University of California
Berkeley, California 94720

T. T. Ng
Department of Aeronautical and
Mechanical Engineering,
University of Notre Dame
Notre Dame, IN 46556

ABSTRACT

Conditional Reynolds stress statistics in a reacting turbulent boundary layer over a strongly heated wall were obtained using two color laser Doppler anemometry technique. Quadrant analysis of the data showed that the reduction in Reynolds stress due to combustion was caused by a decrease in contribution from the bursting event.

INTRODUCTION

Premixed turbulent combustion sustained in a boundary layer over strongly heated flat surface is a combustion configuration which has many engineering and fire safety applications. It is also an unique flow configuration for studying one of the least understood aspects of turbulent combustion -- the mutual interaction between combustion heat release and fluid dynamic turbulence. Since the turbulence flowfield of a fully developed turbulent boundary layer is relatively well-understood, the effects of combustion heat release can be readily identified.

Many recent experimental works on isothermal turbulent boundary layer are emphasized on studying the motion of the large scale turbulence structures, and their relevance to the production of turbulent kinetic energy (see, for example the review by Willmarth (1), Kovasznay (2), and in the book by Hinze (3). These large scale turbulence structures occupy approximately the whole boundary layer thickness, δ_u, and their period of occurrence tend to scale with free-stream velocity U_∞, and δ_u. In the outer region, the features of these structures have been examined using flow visualization (4), conditional sampling (5) and (6). In the inner region close to the wall, the intermittent burst sequence was first shown independently by Kline et.al. (7) and Corino and Brodkey (8) using flow visualization. This burst sequence is characterized by random violent ejection of low momentum fluid from the wall into the overlaying outer region followed by a more quiescent down-sweep of high momentum fluid.

Conditional sampling (9) and conditional statistics (10) in the wall region have shown that during the relatively short duration of the burst and sweep events, substantial contributions are made to the long time average Reynolds stress, $-\bar{\rho}\overline{uv}$. Whereas during a large fraction of the time, contributions to Reynolds stress are very small. In the outer region, intense intermittent contributions to Reynolds stress are also found to be associated with the burst and sweep events. These observations demonstrate a strong interdependency between the outer region large scale structures with the inner region burst sequence, although a direct relationship of the two phenomenon has yet to be established.

The studies of non-isothermal turbulent boundary layer flow with significant density gradients are mainly focussed on compressible turbulent boundary layers with supersonic free stream velocities although there are also a few studies on the subsonic turbulent boundary layers over strongly heated wall. Nicholl (11) reported that the dynamic effects of large density gradients in turbulent boundary layer over the heated floor of a wind tunnel was to create a local wall jet downstream from the leading edge of the heated section. Whereas over the heated roof of the the same wind tunnel, buoyancy stabilized the boundary layer. Rotta (12) deduced analytical profiles for the mean velocity and density distributions in a heated turbulent boundary where the thermal and velocity boundary layers having the same origin. He also derived the friction coefficient and Stanton number from these profiles.

Using Rayleigh scattering and Laser Doppler Anemometry (LDA) Cheng and Ng (13) measured the density and velocity statistics in a turbulent boundary layer with stepwise temperature rise of 800K and free stream air velocity of 20 m/s. They reported that the mean density distribution in the thermal layer followed a logarithmic distribution and that the only observable effect of the strong wall heating on the velocity statistical data was a gradual reduction of Reynolds stress the wall region as the thermal layer grew larger. From the schlieren movies, the thermal structures appeared to be streaks of hot fluids oblique to the wall which moved away into the free-stream as they were convected downstream. The formation of the thermal structures seemed to be cyclic.

Further study of this boundary layer with free stream velocity of 10.5m/s was reported by Ng et.al. (14) They concluded that although the Reynolds stress was reduced near the wall, the reduction was due mainly to the decreased in local mean density. The magnitude of the kinematic Reynolds stresss (i.e. the velocity correlation $-\overline{uv}$) remained relatively unchanged. Ng. et. al. also reported that the stream-wise turbulent kinetic energy diffusion pattern was found to significantly affected by strong wall heating, which suggested that a modification of the boundary layer assumptions would be required to model this flow.

In a subsequent paper, Ng et. al. (15) studied the effects of combustion in this strongly heated turbulent boundary layer with premixed flow of ethylene/air at equivalence ratio, =0.36. Under this condition the reaction zone was found to be totally embedded within the velocity boundary layer. As shown by schlieren observation, combustion reaction occur in discrete flame structures oblique to the wall. The features of these flame structures and their development were very similar to the thermal structures described by Cheng and Ng (18). Which suggested that the motion of the larger scale turbulent structures were predominant in the two flows. As a result of combustion heat release, a modest increase in turbulent kinetic energy was found close to the wall and the streamlines were deflected slightly away from the wall with no acceleration in the stream wise direction. The most significant effect observed was a substantial reduction of Reynolds stress throughout the wall region and in the reaction zone. Unlike the results obtained in the heated boundary layer where the reduction was due primarily to the lowered local mean density, combustion heat release also reduce the magnitude of the velocity correlation $-\overline{uv}$. Since this reduction in Reynolds stress was accompanied by a modest increase in turbulent kinetic energy, our results indicated that other turbulent production mechanism could be important.

The objective of this study is to investigate, in more details, the effects of combustion on the Reynolds stress in the heated and reacting turbulent boundary layers by using a two component LDA system (two color) to make direct instantaneous measurement of two local velocity components. The data are analyzed to obtain conditional statistics of the Reynolds stress for studying the influence of combustion on the turbulence production mechanisms in the turbulent boundary layer. Since the two component LDA system has not yet been widely used for this type of analysis, some measurements are made in isothermal boundary layers to validate the technique by comparing the results with those obtained by others using hot-wire.

EXPERIMENTAL ARRANGEMENTS

Details of the wind tunnel and the computer controlled data acquisition system are described in our earlier papers, (13 to 15) only a brief description is included here. Figure 1 is a schematics of the wind tunnel and flow system. The test section of the wind tunnel is 10 cm square with three different floor treatments, the first segment is lined with sand paper to trip the boundary layer. The second segment has smooth surface which is water-cooled to ensure temperature discontinuity at the junction with the heated section. The heated section is opened and is fitted with nine heating strips which are controlled individually. The wind tunnel is mounted on a three axis computer controlled traverse table for rapid scanning of the boundary layer by the stationary laser probe.

The leading edge of the heated section was used as the origin of the co-ordinated axis with x and y the axial and traverse direction (Figure 2). Measurements were made at thirty y positions across the boundary layer at six axial locations. Experimental conditions for this study included isothermal boundary layers with free stream velocity of 10.5 m/s, heated boundary layers with U at 10.5 m/s both with wall temperature ,T_w, of 1000K, and reacting boundary layer with $U_\infty = 10.5$ m/s, $T_w = 1000$K, using ethylene/air mixture at $\phi = 0.36$.

A Coherent Radiation CW-10 10 watt argon-ion laser supplied the laser source for the four-beam two color LDA system. Typically, the laser was operated at 1.5 to 2.0 watt during the experimental runs. Thermal System Inc. (TSI) transmitting optics were used. The laser beam was separated into blue (488nm) and green (514nm) beams by a dichroic color separator. Each of the two beams was in turn brought into the optical axis by beam displacers and then passed through equal path beam splitters with 5.0cm fixed separation. The four beams were focused by a

600mm focal length lens forming the scattering volume. Scattered bursts were collector by two photomultiplier assemblies placed in the forward scattered direction at approximately $\pm 10^{o}$ from the optical axis. Aluminum oxide seed particles of 0.3 m were introduced into the air flow by a cyclone canister seeder.

The LDA system was arranged to measure the velocity components at $\pm 45^{o}$ with respect to the x axis. The blue beams were used to measure U_1 and the green beams were used to measure U_2 (Figure 2). The main reason for selecting this arrangement was that frequency shifting would not be required for measuring the cross stream velocity component. Using an eight cycle counting criterion in conjunction with the present optical setup, the acceptance angle of the system was $\pm$ 60^{o}. This indicated that the maximum negative cross stream velocity (limited by the blue beams) and the maximum positive cross stream velocity (limited by the green beams) were about $0.27U_{\infty}$. This seemed to be quite adequate to encapsulate the turbulent field in these turbulent boundary layers, as demonstrated in our previous studies where these velocity components were measured separately using a single component LDA system.

The Doppler bursts were analyzed by two TSI 1980A frequency counters. The analog outputs of the counters were digitized by a 12 bit A/D converter operated at a dual sample and hold mode. Random sampling of the data were trigger by a pulse signal from a co-validation circuit which tested the coincidence of the U_1 and U_2 data using the data ready signals sent from the two counters. The criterion for coincidence was that a U_2 data ready signal arrived within 5.0 sec of a U_1 data ready signal. At each measurement position, 4096 pairs of validated velocity data were recorded. Also obtained was the average data rate measured by the time interval between the first and the last validated data pair. In general the data rate from each individual nrequency counter was about 12kHz in the free stream and dropping to 5kHz close to the wall. However, the co-validated data rate was much lower, about 1kHz in the free stream and about 500 Hz close to the wall. Therefore, only 10% of the data could be considered to be simultaneous measurements.

Raw data were stored on magnetic tape and were reduced by the Lawrence Berkeley Laboratory CDC 7600 computer. Mean (U, V) and rms fluctuation (u', v') velocities were deduced in addition to time mean and conditional statistics of Reynolds stress. Also computed were the turbulent kinetic energy (defined here as $k = u'^2 + v'^2$) and the third moments ($\overline{uuu}$, $\overline{uvv}$, $\overline{vuu}$, $\overline{vvv}$). The joint probability density functions (jpdf) at several positions in the reacting and non-reacting boundary layers were also obtained. The conditional Reynolds stress statistics are discussed in this paper. Further descriptions of the other statistical quantities will appear in a subsequent paper.

CONDITIONAL REYNOLDS STRESS

The sorting of Reynolds stress contribution into four quadrants according to the signs of the turbulent velocity components u and v was first introduced independently by Willmarth and Lu (16) and Wallace et.al. (9) This analysis was developed to study the turbulence production mechanisms and also to show the relative importance of the burst and sweep events. The four velocity correlation quadrants are (1) outward interaction, $v>0$, and $u>0$, (2) burst, $v>0$, and $u<0$, (3) inward interaction, $v<0$, $u<0$ and (4) sweep, $v<0$, and $u>0$.

Lu and Willmarth (10) later developed the so-called "hole" analysis to further investigate the large contributions to $-uv$ from each quadrant. In addition to sorting uv contribution into the quadrants, a parameter H, the hole size, is used to prescribe four curves $|uv| = H.u'v'$ (u' and v' are the rms values of the velocity fluctuations). The region where $|uv| < H.u'v'$ is known as the hole region. In the analysis, only contributions larger than $H.u'v'$ are sorted into the quadrants whereas the smaller contributions are sorted into the hole region.

In this study, the contributions from the four quadrants and from the hole region are calculated by the following equation,

$$\frac{\overline{uv}_i(H)}{\overline{uv}} = \frac{1}{\overline{uv}} \sum_{n=1}^{N} \frac{1}{N} \overline{uv}(n)\, S_i(n,H)$$

tion (i.e. 4096). For the four quadrants, S(n,H) satisfies,

$$S_i(n,H) = \begin{cases} 1 & \text{if } uv(n) \quad H.u'v' \text{ and the signs of } u, v \text{ is in the ith quadrant} \\ 0 & \text{otherwise} \end{cases}$$

$$S_h(n,H) = \begin{cases} 1 & \text{if } uv(n) \quad H.u'v' \\ 0 & \text{otherwise} \end{cases}$$

so that

$$\sum_{i=1}^{4} \frac{uv_i}{\overline{uv}} + \frac{uv_h}{\overline{uv}} = 1$$

Since the two color LDA system provides random sampling of the turbulent field, the data are subjected to various LDA biasings. In particular, the velocity bias could cause an uneven distribution of data among the four quadrants. To investigate the possible biasing effect on the quadrant analysis, the number of data pairs falling into each quadrant is also computed. The results show that in the free-stream, approximately 25% of the total number of data pairs are within each quadrant. In the isothermal layer, and in the wall region the number of data is slightly higher in the two negative quadrants 2 and 4 (about 30%) than in the other two quadrants. Similar results are observed in the heated and reacting layers indicating that our data are not significantly affected by velocity bias.

RESULTS

Shown in Figure 3 is an example of the fractional uv contribution to the four quadrants as a function of hole size. As can be seen, contribution from the burst and sweep events are significantly higher than those in the inward and outward interaction events. Since contributions from the burst and sweep events are negative, their contributions to Reynolds stresss are positive. As the hole size increase, contributions from quadrants 1, 3, and 4 fall off rapidly and at $H>3.0$ the only contribution to uv is from the burst event quadrant 2. This shows that the ejection of low momentum fluid from the wall region can make instantaneous Reynolds stress contribution which is several times higher than the time mean Reynolds stress. At other locations, for example closer to the wall, contribution from quadrant 4 becomes more significant. At $Y/\delta_u = 0.1$, the contributions from quadrants 2 and 4 are comparable.

These results are in excellent agreement with those obtained by Lu and Willmarth (10) using hot-wire anemometry indicating that the two color LDA technique is fully capable of providing reliable instantaneous Reynolds stress data which can be used for conditional analysis.

Reynolds stress profiles at six axial locations across the isothermal layer are shown in Figure 4. These data are normalized by the stress velocity δ_u obtained by fitting the mean U profile with the logarithmic law of the wall. The distance above the wall is normalized by the velocity boundary layer thickness δ_u ($y=\delta_u$ at $U/U_\infty=0.99$). Also shown is the typical Reynolds stress distribution in a fully developed isothermal turbulent boundary layer over a smooth wall. In comparison to the results of our previous measurements using a single component LDA system, the present data are less scattered and in the region $0.2<y/_u<0.8$, compare better with the typical profile.

Conditional Reynolds stress associated with the profiles of Figure 4 are shown in Figure 5. To obtain a a basis of comparison between these results with those measured in the heated and reacting layers, the uv contributions are not normalized by the local Reynolds stress as in the works of Willmarth and Lu (16) and Wallace et.al. (9) Again, the dominance of the burst and sweep event in uv contribution is shown by these conditional Reynolds stress results. The distributions in each quadrant appear to be self similar as in the mean Reynolds stress profiles.

Results measured in the heated layer are shown in Figure 6 and 7. These results are the kinematic Reynolds stresses $-\overline{uv}$ shown without weighted by the local mean density to give the Reynolds stress $-\bar{\rho}\overline{uv}$. As can be seen, the heated layer profiles are not significantly different than those shown in Figure 4 for the isothermal layer. except for a slight decrease in in the wall region at x>125.0mm. The similarity between the profiles for the isothermal and heated layers demonstrates that the reduction of Reynolds stress in the heated case is due mainly to the decrease in local mean density near the wall region and not to a decrease in the velocity correlation.

In Figure 7, conditional profiles obtained for the four quadrants are also similar to those shown in Figure 5. At x=155.0 and 182.0mm, a slight decrease in $\overline{uv}_2$ is apparent near $y/\delta_u = 0.1$. This decrease corresponds to the decrease in mean $-\overline{uv}$ shown in Figure 6. Since in a heated layer, the bursting event consists of ejection of low momentum hot fluids from the wall, this decrease of $\overline{uv}_2$ could possibly indicate the ejected fluids become less correlated as the thermal layer becomes larger downstream from the origin.

Kinematic Reynolds stress profiles in the reacting layer are shown in Figure 8. As observed in our previous paper (15), $-\overline{uv}$ measured in the reaction zone is greatly reduced. Since local mean density is also reduced, the Reynolds stress is significantly smaller as compare to the isothermal and heated layers. At x=35.0mm, close to the origin of the heated section, $-\overline{uv}$ increases to its maximum at $y/\delta_u 0.3$, at $0.1<y/\delta_u<0.3$ a slight decrease is shown, and at $y/\delta_u<0.1$, $-\overline{uv}$ increases again towards the wall. The feature of this profile is consistent with our previous measurement. Further downstream at x > 155.0mm, maximum $-\overline{uv}$ occur at $y/\delta_u \cong 0.6$ and then decrease towards the wall region.

The conditional profiles for the reacting layer are shown in Figure 9. Here, the profiles are quite different than those shown in Figures 5 and 7. In particular, the $-\overline{uv}_2$ profiles show a significant decrease. Some features of the $-\overline{uv}_2$ profiles seem to correspond to the those of the mean Reynolds stress profiles showing that the mean Ryenolds stress level is mostly dominated by $-\overline{uv}_2$. For example at x=35.0mm, a maximum is reached at y/δ_u=0.3 then a decrease is shown towards the wall, follows by an increase at $y/\ _u$=0.2. At x=125.0mm, $-\overline{uv}_2$ reaches $-.1(m/s)^2$ at $y/\delta_u \cong 0.6$ and drops to $-0.025(m/s)^2$ at the wall. The $-\overline{uv}_4$ profiles are more scattered than those of Figures 5 and 7. However, near the wall region, the magnitude of $-\overline{uv}_4$ is still quite comparable to those of the isothermal and reacting layers.

From these results, it can be concluded that the reduction in velocity correlation observed in the reacting layer is due mainly to a significant reduction in $-\overline{uv}_2$ while contributions from the other three quadrants remain relatively unchanged. As suggested by the cyclic development of the flame structures shown on schlieren movies, the overall fluid motion in the region close to the wall would consist of in-rushing (sweep) of cold unburnt reactant from the outer region towards the heated wall and ejection (burst) of hot reacting fluid into the outer region. Since the inrushing fluids obtain their energy from the mean flow, their contribution to the kinematic Reynolds stress would not seem to be greatly affected by combustion. In contrast, the ejected hot fluids originate from the heated wall where the mixing of hot burnt fluids and cold unburnt fluids occurs. The conditional statistics show that the contributions due to bursting event are significantly less comparing to the isothermal and heated cases meaning that the bursting events become less violent and less correlated. Since bursting is the most significant turbulence production mechanism in the turbulent boundary layer, the turbulent kinetic energy should show a reduction due to combustion. On the contrary, as shown by the u' and v' results, the turbulent kinetic energy near the wall is actually slightly higher than the levels measured in the isothermal and heated layers.

One possible explanation for the decrease in kinematic Reynolds stress is that combustion induces vigorous and relatively random flow acceleration. This may significantly alter the turbulent structures in the ejected fluids causing it to be less correlated. But at the same time, combustion induced local flow acceleration which could increase the fluctuation intensities so that the overall turbulent kinetic energy level can become higher. Another possible explanation for the decrease in $-\overline{uv}_2$ is that the high viscosity in the hot fluid near the wall region could reduce the intensity of the interaction of the unburnt and the burnt fluids which follows the sweep event. Therefore the subsequent burst event could become less violent. To gain better understand the influence of combustion on the turbulence production mechanisms, and also the interrelationship between the combustion induced velocity fluctuation and the large scale turbulence structures, measurement of other correlation parameters such as the density and velocity correlation and spatial density correlation would be most useful. These studies will be carried-out in the future.

SUMMARY

A two color LDA system was used to study the isothermal, heated and reacting turbulent boundary layers. The data were reduced to obtain conditional Reynolds stress statistics. In the isothermal turbulent boundary layer, the results were in excellent agreement with those obtains by others using hot-wire anemometry. The results for the heated layer were not significantly different from those measured in the isothermal case. Significant reduction of the velocity correlation was found in the reacting layer. The conditional statistics shown that this reduction was due to a decrease in the contributions from the burst events. Since the ejection of low momentum fluids from the wall region during the burst event is the most significant turbulent production mechanism in the turbulent boundary layer, our results indicated that the ejected fluids in the reacting layer became less violent and less correlated.

ACKNOWLEDGEMENTS

This work was supported by the Director, Office of Energy Research, Office of Basic Energy Sciences, Chemical Sciences Division of the U. S. Department of Energy under Contract No. DE-AC-03-76SF00098. The authors should like to thank Dr. F. Robben and Prof. L. Talbot for their continued support and advice.

LITERATURE CITED

1. Willmarth, W. W., Advances in Applied Mechanics, 15, p. 159 (1975).

2. Kovasznay, L. S. G., Proc. 5th Biennial Symp. on Turbulence, Princeton Science Press (1977).

3. Hinze, J. O., Turbulence, McGraw Hill, New York (1975).

4. Falco, R. E., Physics of Fluids, 20, S248 (1977).

5. Kovasznay, L. S. G., Kibens, V., and Blackwelder, R. F., J. Fluid Mech., 41, p. 283 (1970).

6. Raupach, M. R., J. Fluid Mech., 108, p. 363 (1981).

7. Kline, S. J., Reynolds, W. C., and Schwaub, F. A., J. Fluid Mech., 30, p. 741 (1967).

8. Corino, E. R., and Brodkey, R. S., J. Fluid Mech., 37 part 1, p. 1 (1969).

9. Wallace, J. M., Eckelmann, H., and Brodkey, R. S., J. Fluid Mech., 54, p. 39 (1972).

10. Lu, S. S., and Willmarth, W. W., J. Fluid Mech., 60, P. 481 (1973).

11. Nicholl, C. I. H., J. Fluid Mech., 40, 2, p. 361 (1970).

12. Rotta, J. C., Warme-und-Straffubertragung, 7, p. 133 (1974).

13. Cheng, R. K., and Ng, T. T., Phy. of Fluid, 25, 8, p. 1392 (1982).

14. Ng., T. T., Cheng, R. K., Robben, F., and Talbot, L., Int'l Symp. on Appl. of Laser Doppler Anemometry to Fluid Mech., in press (1983).

15. Ng, T. T., Cheng, R. K., Robben, F. and Talbot, L., 19th Symp (Int'l) on Combustion, The Combustion Institute, p. 359 (1983).

16. Willmarth, W. W. and Lu, S. S., J. Fluid Mech., 55, p. 481 (1971).

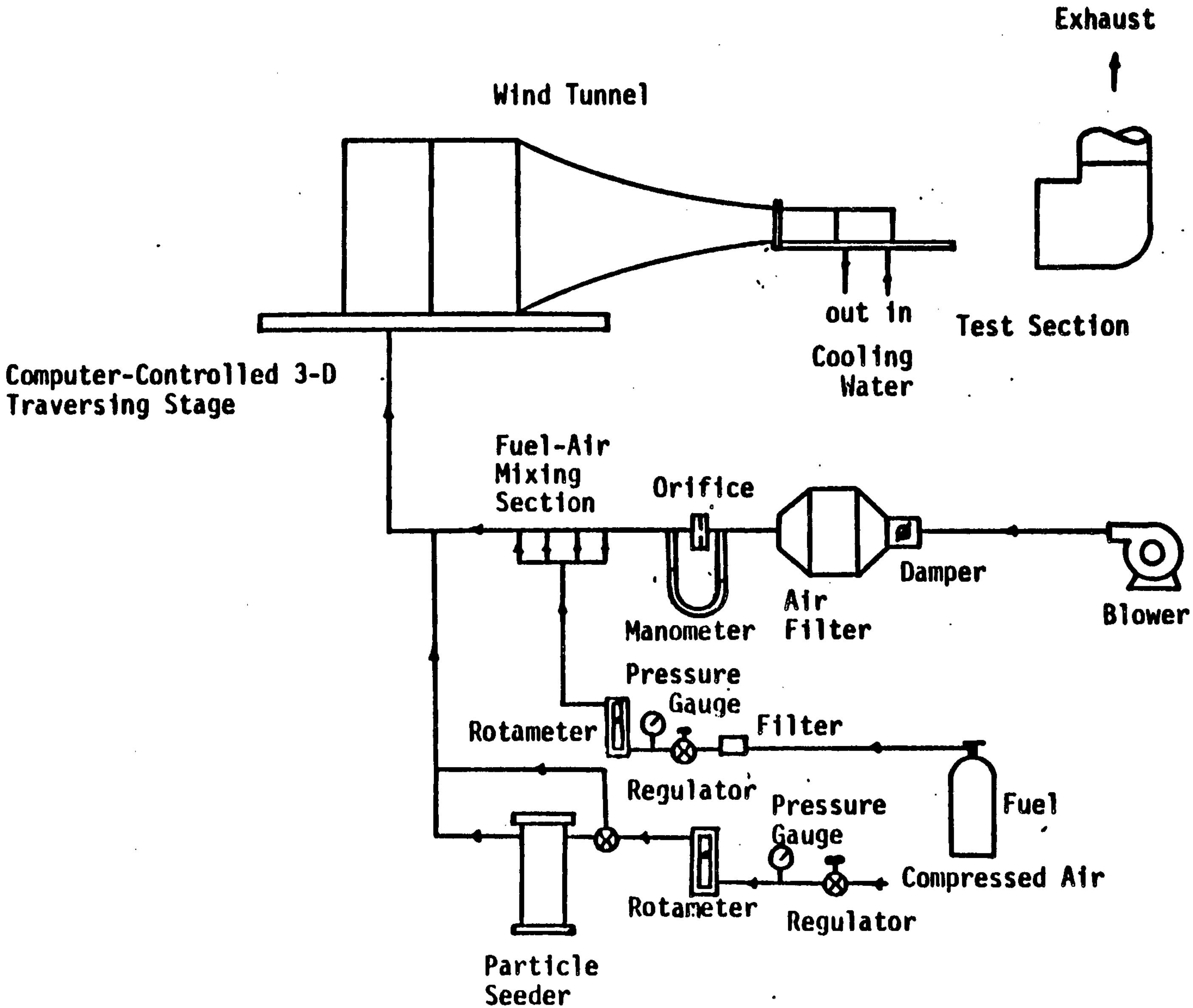

Fig. 1 Schematic Diagram of the Flow System

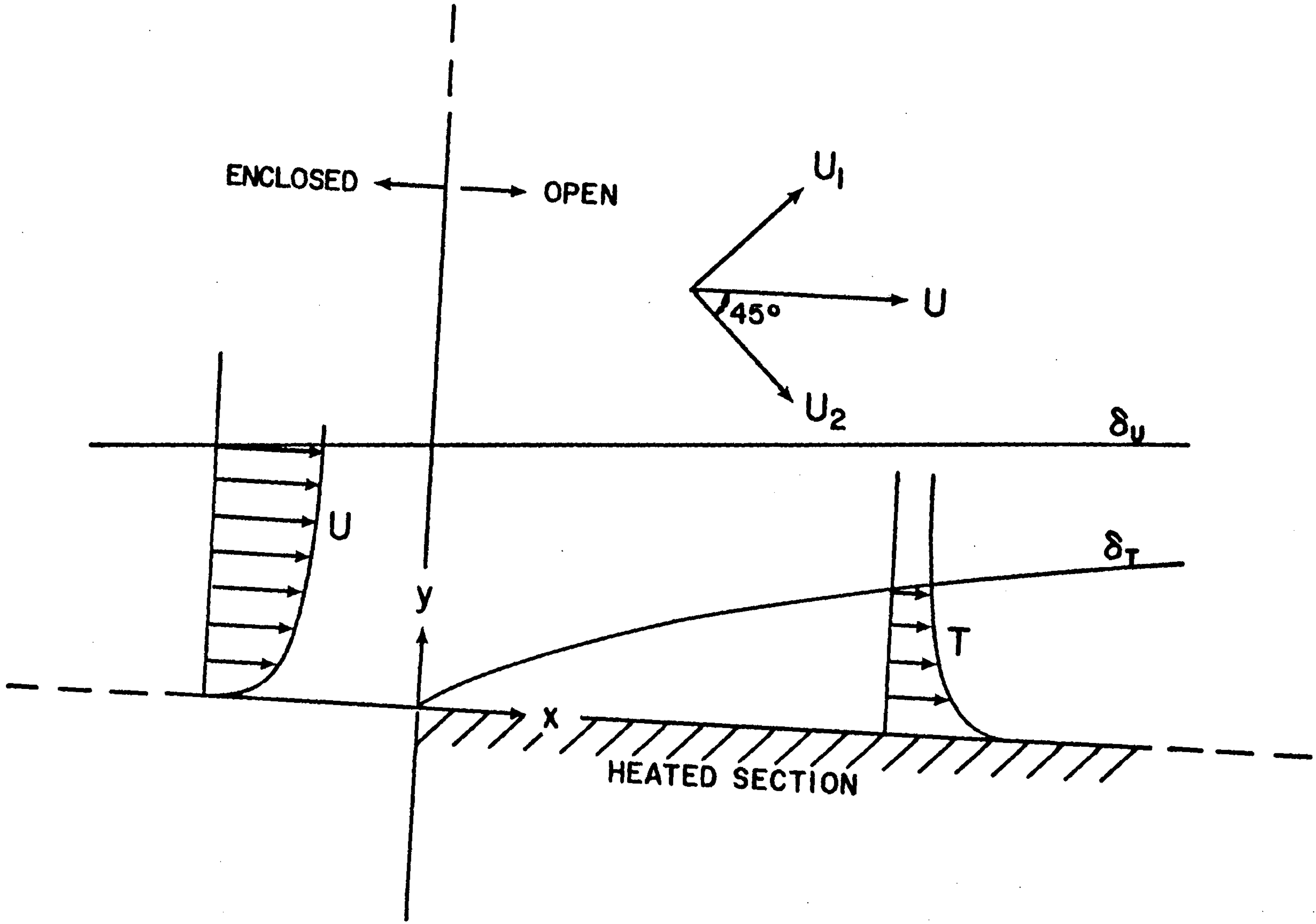

Fig. 2 Co-ordinate system and orientations of the velocity components in the test section.

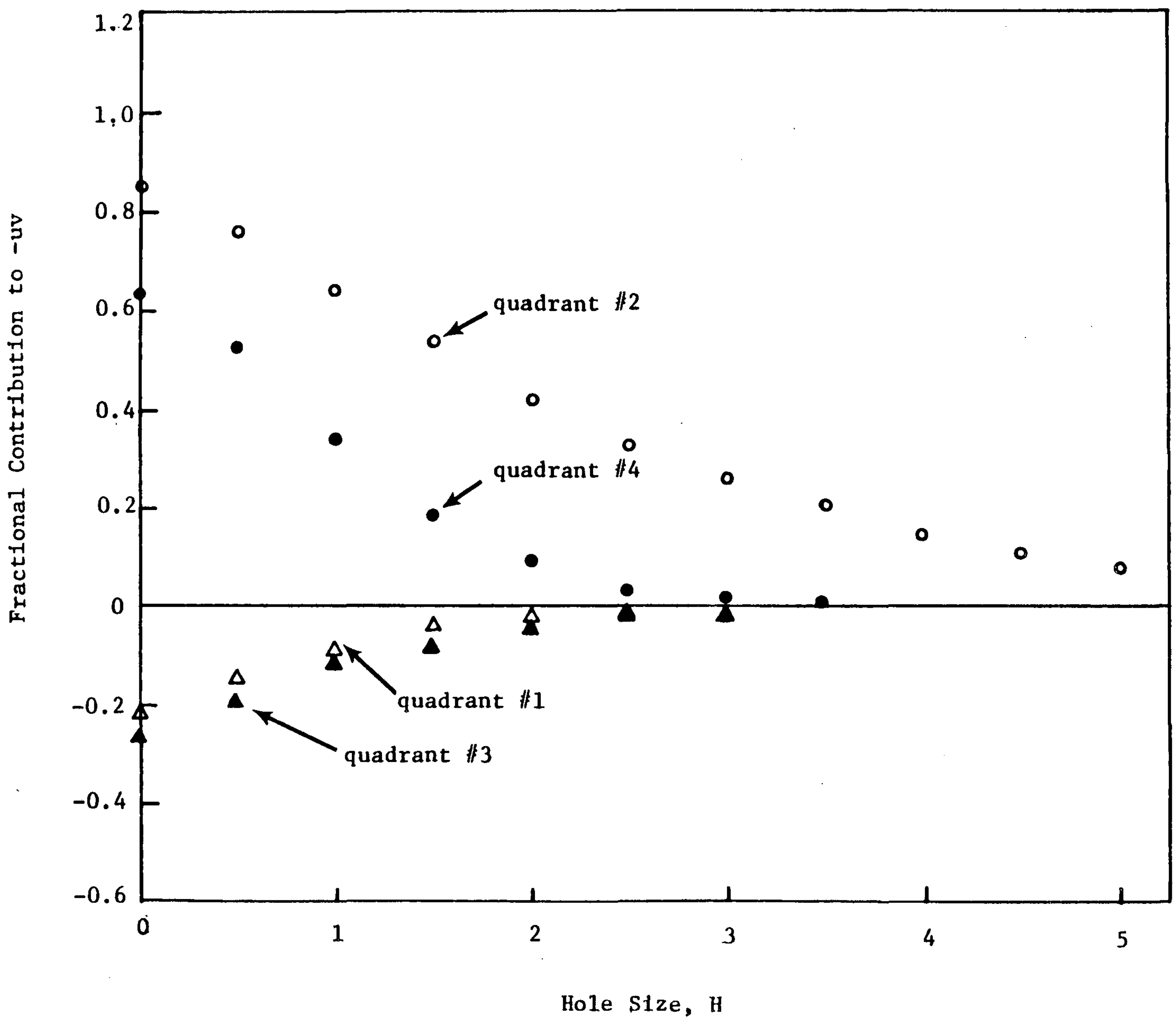

Fig. 3 Fractional contributions from the four quadrants in the isothermal turbulent boundary layer at $y/\delta_u = 0.7$.

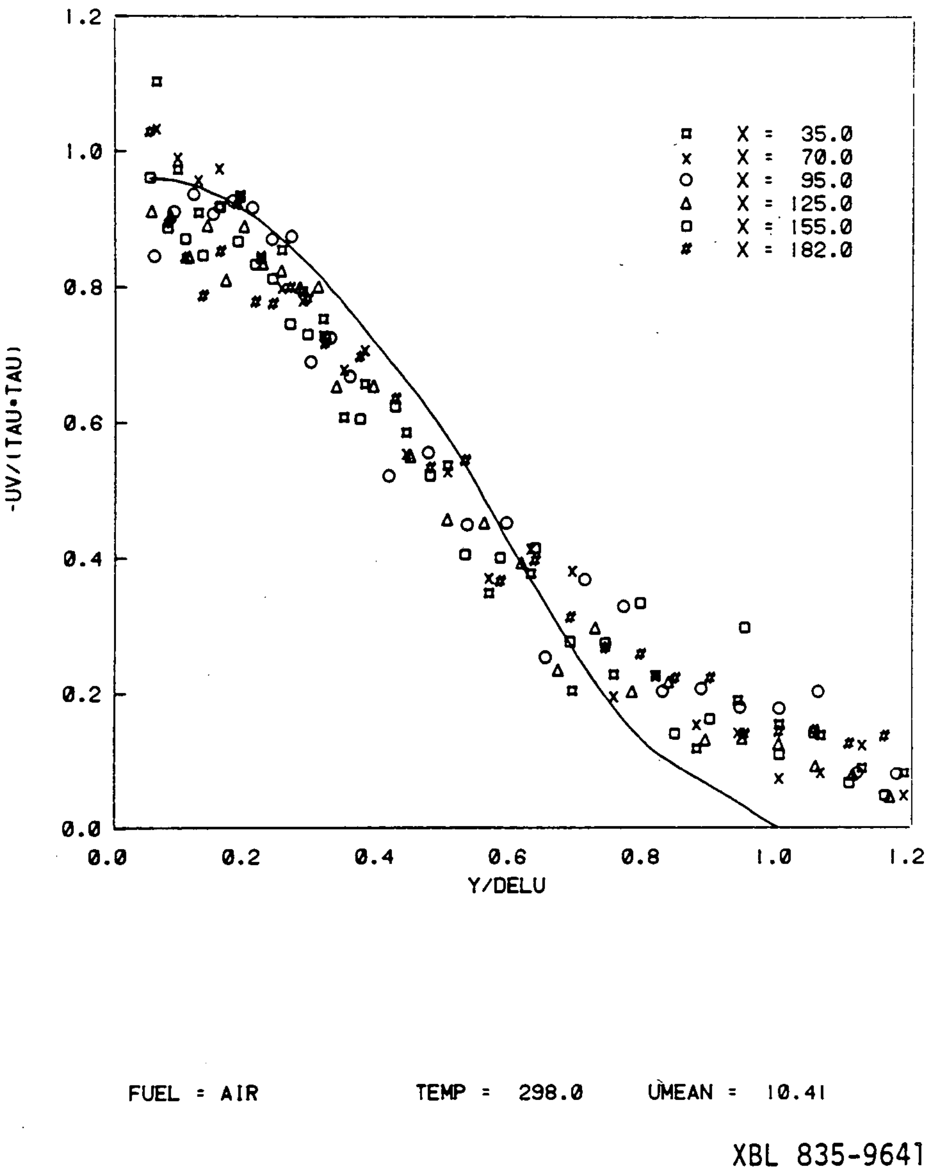

Fig. 4 Reynolds stress profiles in the isothermal turbulent boundary layer.

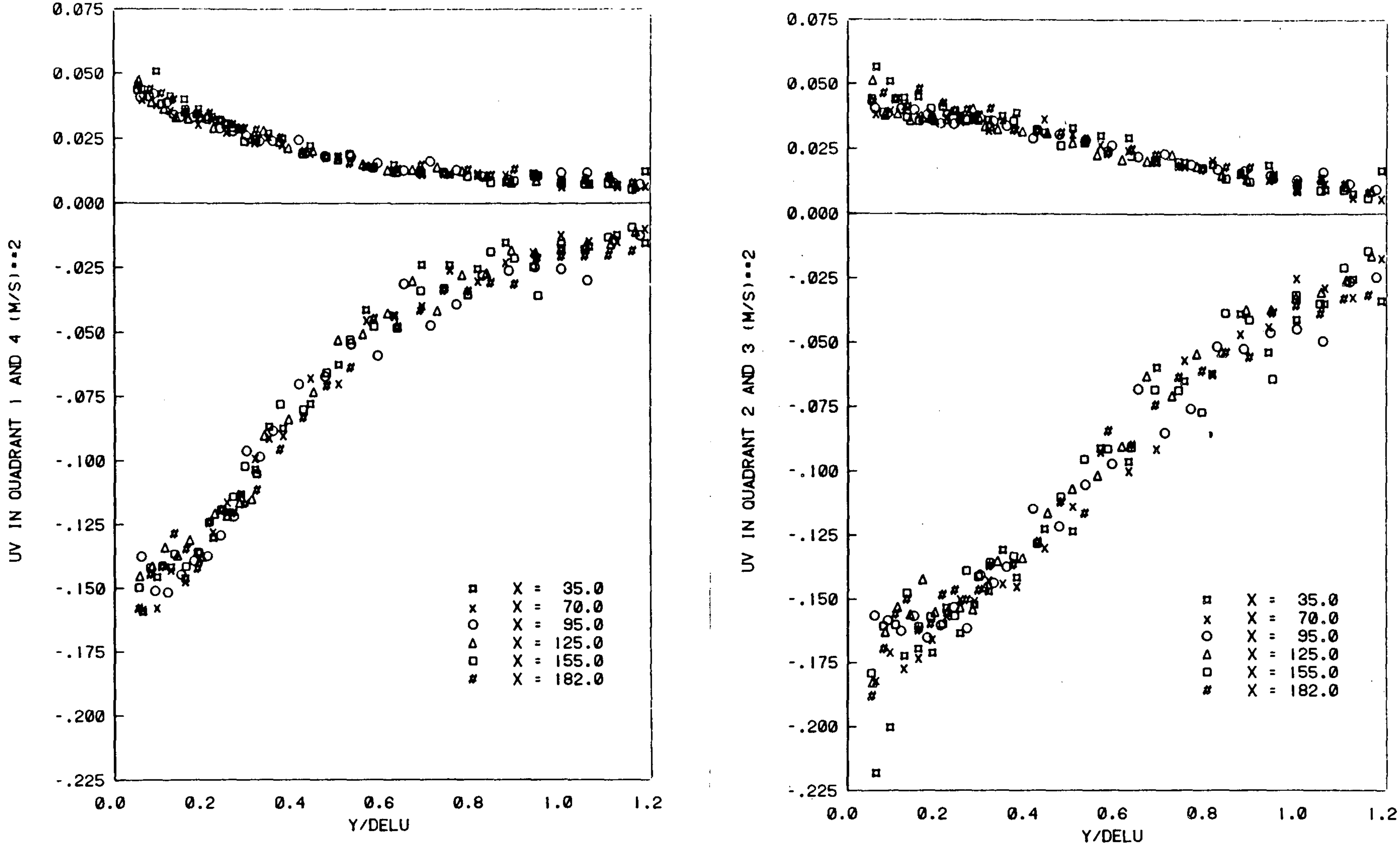

Fig. 5 Conditional velocity correlation profiles in the isothermal turbulent boundary layer.

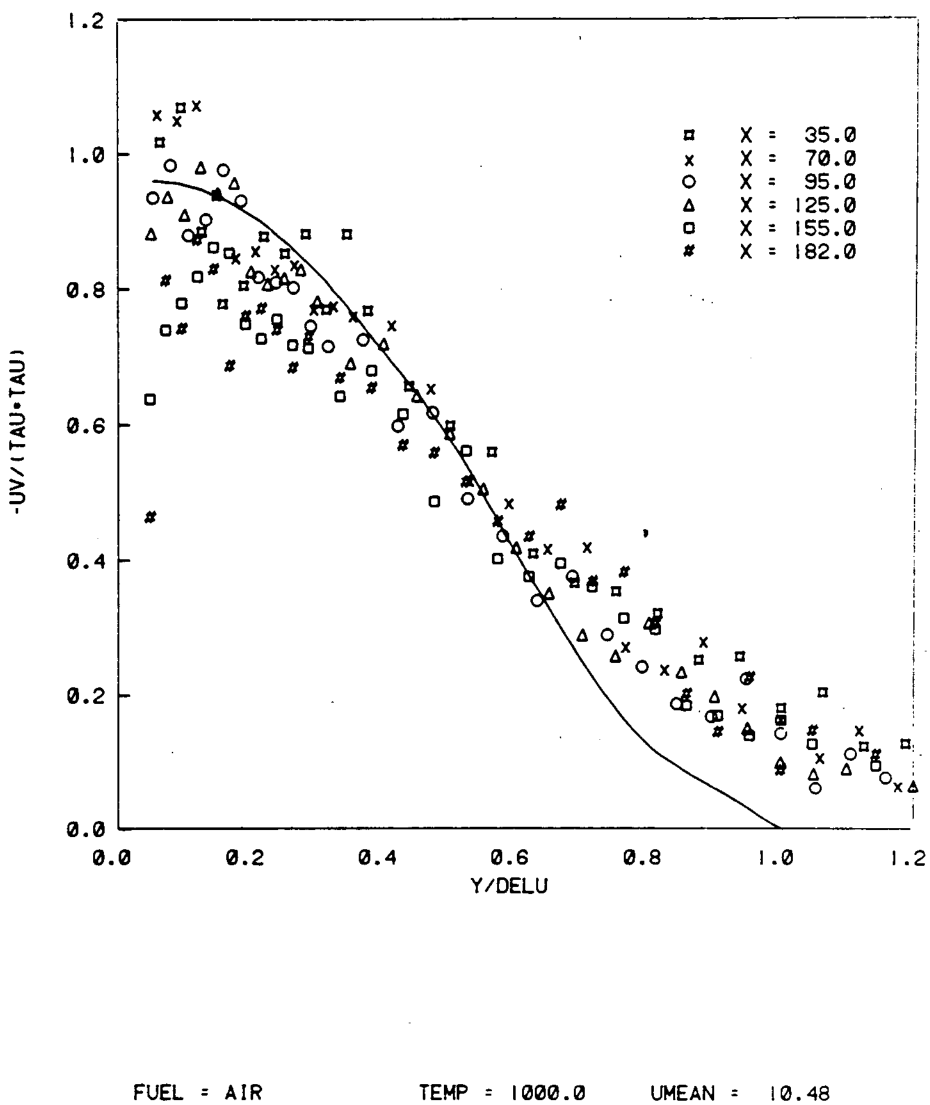

XBL 835-9642

Fig. 6 Velocity correlation profiles in the heated turbulent boundary layer.

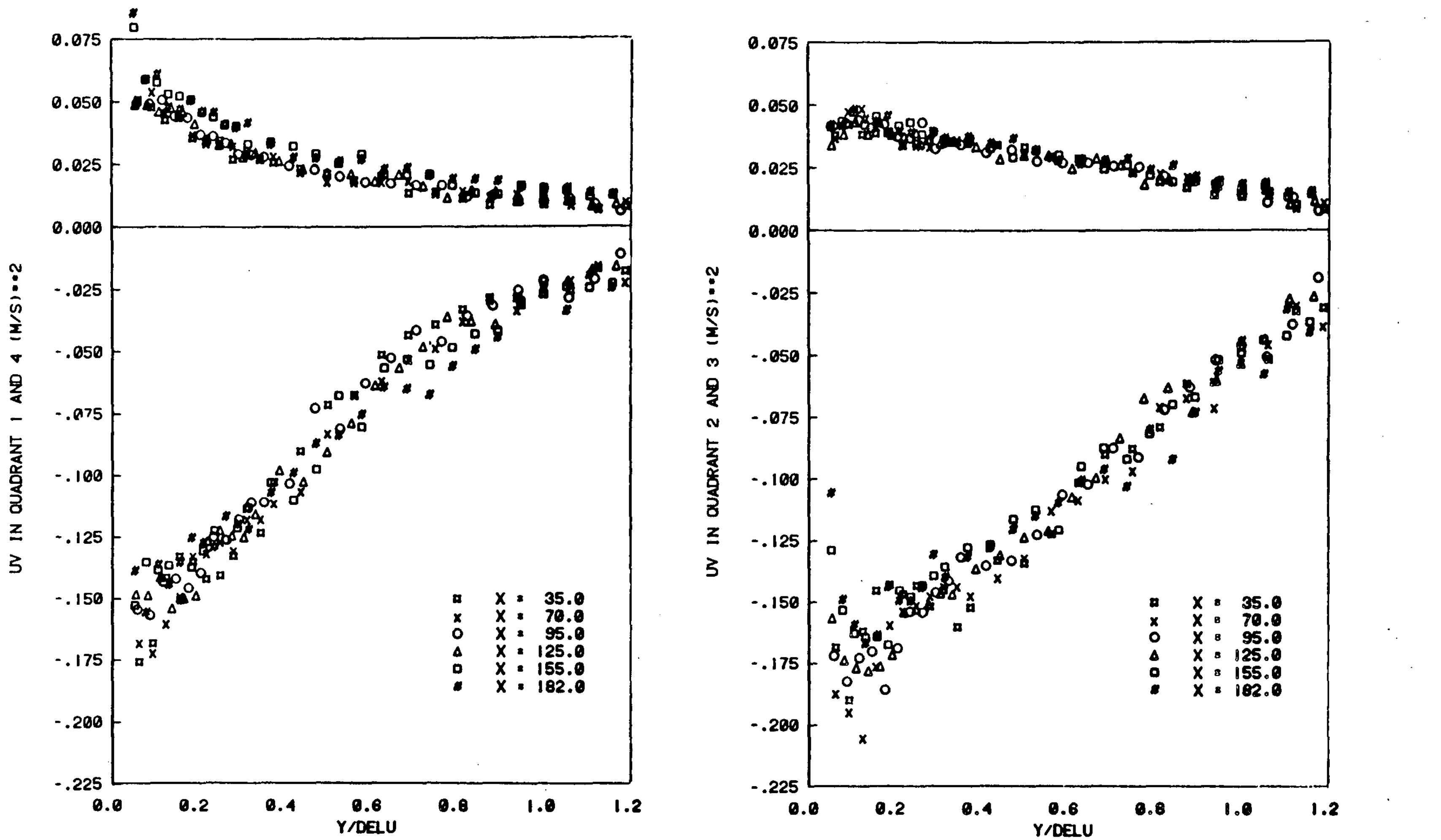

Fig. 7 Conditional velocity correlation profiles in the heated turbulent boundary layer.

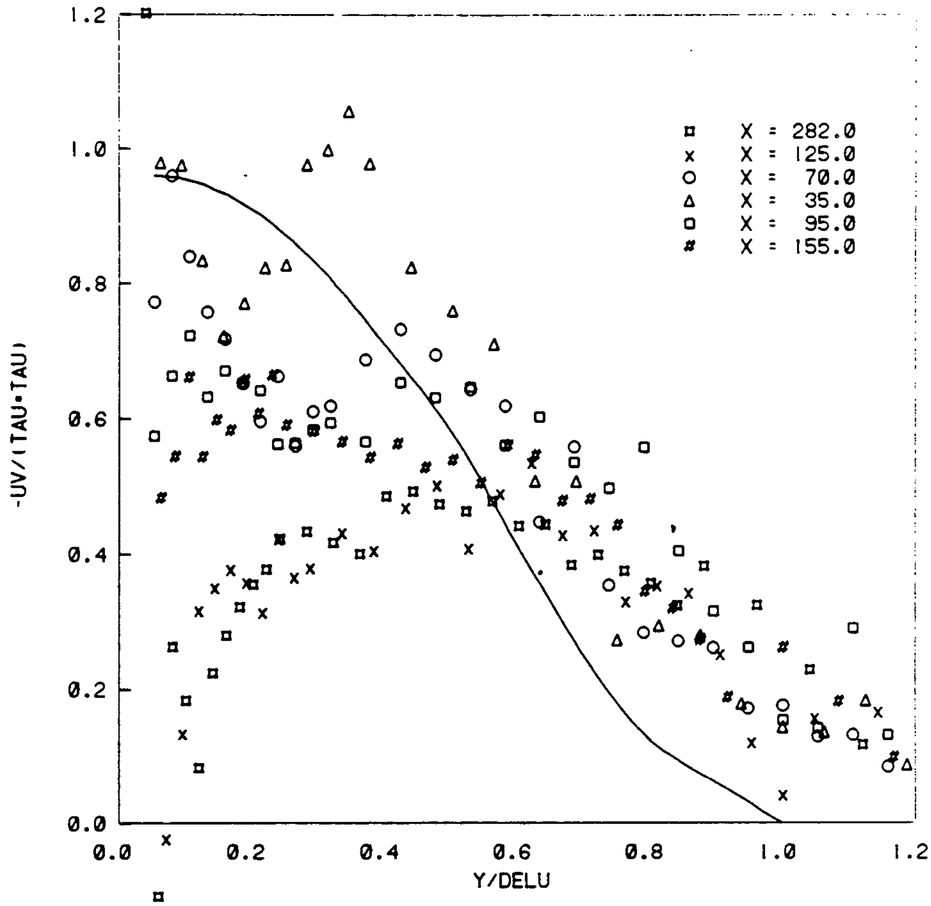

Fig. 8 Velocity correlation profiles in the reacting turbulent boundary layer.

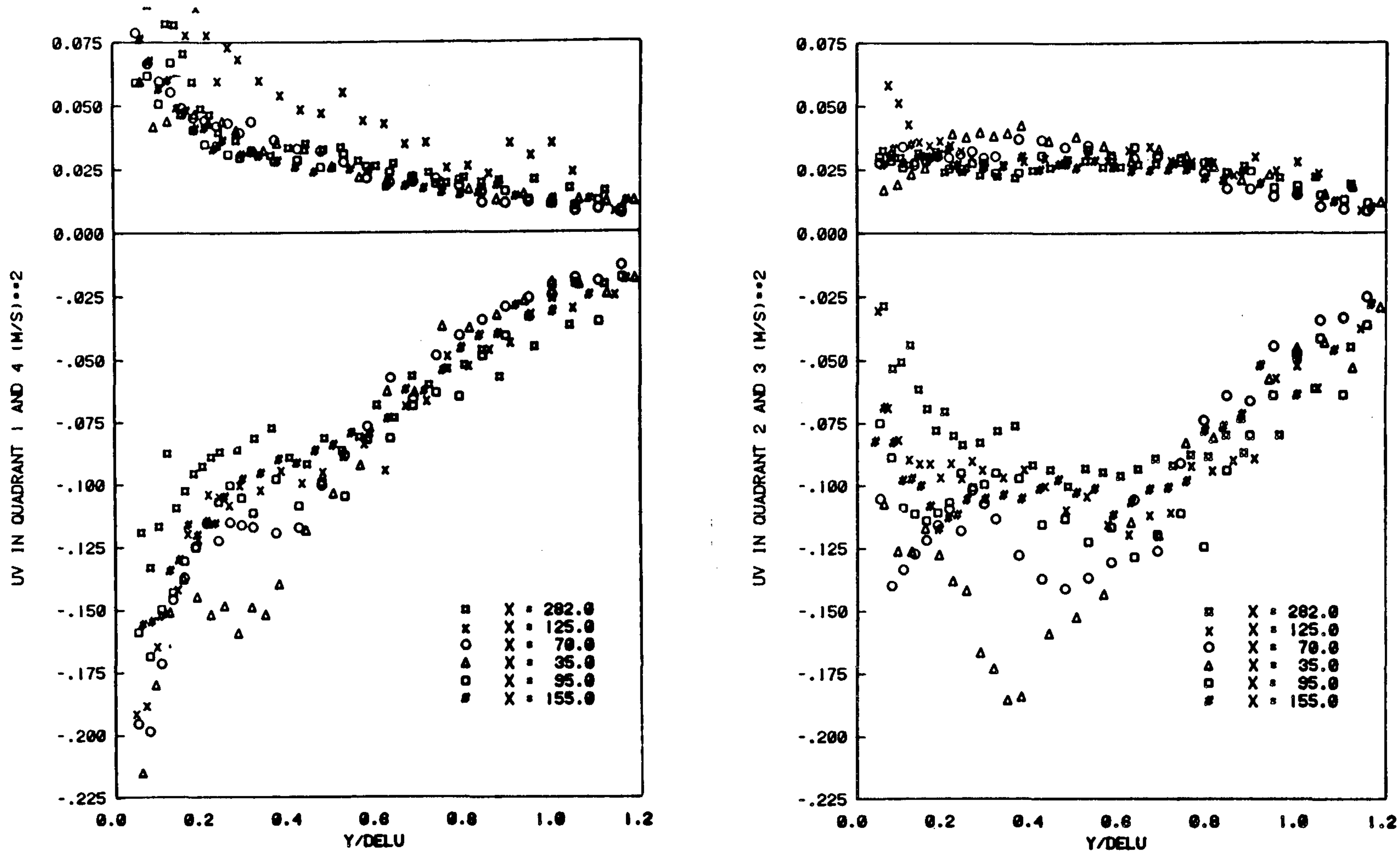

Fig. 9 Conditional velocity correlation profiles in the reacting turbulent boundary layer.

TECHNICAL INFORMATION DEPARTMENT
LAWRENCE BERKELEY LABORATORY
UNIVERSITY OF CALIFORNIA
BERKELEY, CALIFORNIA 94720